Chapter 3

Oxygen and carbon stable isotope records of marine vertebrates from the type Maastrichtian (Late Cretaceous)

Renée Janssen, Remy R. van Baal, Jeroen H.J.L. van der Lubbe, Anne S. Schulp, John W.M. Jagt, Hubert B. Vonhof

Based on data previously published in *van Baal, R. R., Janssen, R., van der Lubbe, H. J. L., Schulp, A. S., Jagt, J. W., & Vonhof, H. B. (2013). Oxygen and carbon stable isotope records of marine vertebrates from the type Maastrichtian, The Netherlands and northeast Belgium (Late Cretaceous). Palaeogeography, Palaeoclimatology, Palaeoecology, 392, 71-78.*

Abstract

Here we present the stable isotope compositions of structural carbonate ($\delta^{13}C$ and $\delta^{18}O_{sc}$) and phosphate ($\delta^{18}O_p$) in the teeth of ten late Maastrichtian and early Paleocene neoselachian (shark and ray) species, as well as carapace bone of the late Maastrichtian marine turtle *Allopleuron hofmanni*. All specimens were excavated from the type area of the Maastrichtian Stage in the southeast Netherlands and northeast Belgium. A lack of correlation between neoselachian $\delta^{18}O_p$ and $\delta^{18}O_{sc}$ values, and offset with modern shark $\delta^{18}O_{sc}$ values suggests diagenetic alteration of structural carbonate oxygen. Neoselachian $\delta^{18}O_p$ values (16.9 to 25.0‰) are comparable to extant shark $\delta^{18}O_p$ values. Based on the median value of 22.3‰ for these samples we calculate a paleoseawater temperature of 19.7°C, which is in good agreement with expected temperatures for this region in the Maastrichtian. The total range in $\delta^{18}O_p$ values is interpreted to reflect both temperature variation and spatial variation in seawater $\delta^{18}O_w$. There is an offset between dentin and enamel $\delta^{13}C$ values in the fossil neosalachian teeth, similar to the offset found in modern shark teeth. Overall more enriched $\delta^{13}C$ values for the Maastrichtian-Paleocene dataset suggest relatively high $\delta^{13}C$ values at the base of the food chain. Based on the carbon isotope values of *A. hofmanni* bone we cannot exclude the possibility that this species engaged in frequent long-duration dives, but in light of realistic diet $\delta^{13}C$ values it is deemed more likely that the $\delta^{13}C$ bone values in this marine turtle were not significantly affected respired CO_2 accumulation during long dives. A carnivorous diet

and a herbivorous (seagrass) diet for *A. hofmanni* are both feasible possibilities given the measured $\delta^{13}C$ values, although the latter option would require relatively low seagrass $\delta^{13}C$ values compared to that of extant species.

3.1 Introduction

During the latest Cretaceous (c. 67–66 Ma) the southeast Netherlands and northeast Belgium were covered by a shallow subtropical sea (Felder, 1994; Schiøler et al., 1997; Mulder et al., 2005; Jagt and Jagt-Yazykova, 2012). The highly fossiliferous biocalcarenites of the ENCI–Heidelberg Cement Group quarry in Maastricht and various other quarries (both active and defunct) document the complete upper Maastrichtian and the lower and middle Danian (lower Paleocene) (Felder, 1975, 1995; Jagt et al., 1996; Schiøler et al., 1997). A wide range of vertebrate fossils has been recovered from these marine strata, including mosasaurid squamates (Dortangs et al., 2002; Schulp, 2006), elasmosaurid plesiosaurs (Schulp et al., 2016), and cheloniid turtles (Mulder, 2003). Also present are rare remains of terrestrial taxa such as hadrosaurid dinosaurs (Jagt, 2003), birds (Dyke et al., 2008) and mammals (Martin et al., 2005). Shark and ray teeth are particularly abundant at several levels within this sequence, but little is known of the paleoecological and paleoenvironmental conditions under which these vertebrates thrived. Stable isotope analyses of these fossils may help elucidate such boundary conditions.

Here, we analyze the stable isotope compositions of late Maastrichtian and early Paleocene neoselachian (shark and ray) teeth and a carapace fragment of a marine turtle, *Allopleuron hofmanni* (Gray, 1831). Two fractions of biogenic apatite were targeted in these analyses: oxygen in phosphate ($\delta^{18}O_p$) and carbon and oxygen in structural carbonate ($\delta^{13}C$ and $\delta^{18}O_{sc}$).

3.2 Materials and methods

3.3.1 Sample materials

The biogenic apatite material analyzed includes a total of 44 shark and ray teeth from the collections of Natuurhistorisch Museum Maastricht in the Netherlands (Table 3.1). These were collected from various levels within the Maastrichtian Gulpen and Maastricht Formations, as well as the early Paleocene Houthem Formation. The neoselachian taxa include small squaliformes (dogfish sharks) with their specialized cutting type dentition, often occurring in bottom waters and presumably preying on fish, crustaceans and cephalopods. The collection

also includes much larger-sized lamniformes (mackerel sharks), which are medium to large-sized pelagic apex predators eating a wide variety of prey, and myliobatiformes (rays).

Furthermore, we analyzed a carapace fragment of *A. hofmanni,* also from the collections of the Natuurhistorisch Museum Maastricht (specimen no. NHMM 2008 137). This marine turtle has an uncertain phylogenic position and is found solely in the Maastrichtian type area (Mulder, 2003; Janssen et al., 2011; Chapter 2 of this thesis).

Table 3.1 Shark and ray species analyzed in the present study (including the number of specimens analyzed), with assignment to family and pertinent references.

species	family	reference
Centrophoroides appendiculatus (n = 2)	Squalidae	Herman (1977), Cappetta (1987)
Cretalamna appendiculata pachyrhiza (n = 1)	Cretoxyrhinidae	Herman (1977)
Palaeohypotodus bronni (n = 19)	Odontaspididae	Herman (1977)
Anomotodon sp. (n = 1)	Mitsukurinidae	Herman (1977), Cappetta (1987)
Serratolamna serrata (n = 2)	Serratolamnidae	Welton and Farish (1993)
Carcharias sp. (n = 2)	Odontaspididae	Cappetta (1987)
Squalicorax pristodontus (n = 4)	Anacoracidae	Welton and Farish (1993)
Pseudocorax affinis (n = 7)	Anacoracidae	Herman (1977)
Rhombodus binkhorsti (n = 1)	Rhombodontidae	Welton and Farish (1993)
Ganopristis leptodon (n = 1)	Sclerorhynchidae	Herman (1977)

3.3.2 Experimental methods

To minimize the potential impact of diagenesis on our dataset, we made an effort to sample tooth enamel rather than the more porous and less mineralized dentin (Kolodny and Raab, 1988; Wang and Cerling, 1994; Picard et al., 1998; Sharp et al., 2000; Lécuyer et al., 2003; Pucéat et al., 2003; Stanton Thomas and Carlson, 2004). However, in the case of very small teeth, dentin may have been sampled to some degree. These specimens are marked with an asterix in Table 3.2, and are labeled 'enamel + dentin' in the figures.

Prior to isotope analysis, tooth samples were soaked in a 1 M acetic acid solution for 45 minutes in order to remove secondary $CaCO_3$, and subsequently washed with Milli-Q water (Bocherens et al., 1996). Approximately 7 mg of powdered sample material was taken from each tooth using a handheld dentist drill. The turtle carapace fragment was embedded in epoxy and cut dorsoventrally. We sampled two separate growth incremental series, one in the cortical (compact) and one in the cancellous (spongy) bone, using a Merchantec MicroMill for

samples used in $\delta^{13}C$ and $\delta^{18}O_{sc}$ analyses (~1 mg) and a handheld dentist drill for larger samples (~7 mg) for $\delta^{18}O_p$ measurements.

Acid-digestion of the structural carbonate fraction

Carbon and oxygen isotope values of the structural carbonate were measured through acid-digestion as first described in McCrea (1950). Apatite powder samples of ~0.4 mg were placed in exetainer vials, which were then flushed with pure (99.99%) helium gas. Adding orthophosphoric acid and leaving the samples to digest for at least 24 hours at 45°C ensured quantitative dissolution of the structural carbonate (McCrea, 1950). Subsequently, multiple samples of the generated CO_2–He mixture gas were analyzed using a Thermo Finnigan GasBench II preparation device interfaced with a Thermo Finnigan Delta Plus mass spectrometer. For both $\delta^{13}C$ and $\delta^{18}O_{sc}$, the uncertainties were 0.13‰, as determined by multiple analyses of VICS (VU In-house Carbonate Standard; normalized to NBS 18, 19 and 20) placed in the same sample run. Data for $\delta^{13}C$ are reported relative to the Vienna Peedee Belemnite (VPDB) standard, while $\delta^{18}O_{sc}$ data were recalculated relative to Vienna Standard Mean Ocean Water (VSMOW) using equation 1 (Friedman and O'Neil, 1977).

$$\delta^{18}O_{VSMOW} = 1.03086 \times \delta^{18}O_{VPDB} + 30.86 \quad \text{(equation 1)}$$

High-temperature reduction of the phosphate fraction

Biogenic apatite was converted to silver orthophosphate (Ag_3PO_4), following techniques described by Dettman et al. (2001). To verify the absence of fractionation during the conversion of biogenic apatite to Ag_3PO_4, two standard materials were included in each sample batch: NIST SRM 120c (Florida phosphate rock) and an in-house standard consisting of a powdered *Megaselachus megalodon* tooth (23.70‰). Samples and standards were then analyzed alternately using a Thermo Finnigan Thermal Conversion Elemental Analyzer (TCEA) interfaced with a Finnigan Delta Plus XP gas source mass spectrometer (Vennemann et al., 2002).

Values for $\delta^{18}O_p$ were standardized to the Vienna Standard Mean Ocean Water (VSMOW) scale assuming a value of 22.58‰ $\delta^{18}O_p$ for NIST SRM 120c (following Vennemann et al., 2002; Joachimski et al., 2009; Pucéat et al., 2010). Different $\delta^{18}O_p$ values have been reported for this standard: It is thought that the uncertainty around the exact value for NIST SRM 120c arises from differences in the chemical protocols used to extract PO_4 and the technique and temperature used in the oxygen isotope ratio measurements (Vennemann et al., 2002; Pucéat et al., 2010; Chang and Blake, 2015). Work by Chenery et al. (2010), Halas et

al. (2011), and others suggest that its value may be as low as 21.7‰. Vennemann et al. (2001) used wet chemistry and measurement techniques similar to our study, but found a value of 22.1‰ $\delta^{18}O_p$. Because it is not clear to which value should ideally be assumed when working with the combination of techniques we used, and because the results presented here have been published before (van Baal et al., 2013), we will here retain the value of 22.58‰ $\delta^{18}O_p$ originally used. Because of the offset in NIST SRM 120c values and the similarity in chemistry and measurement techniques, comparison between our dataset and the Vennemann et al. (2001) may ideally involve a transposition of 0.5‰. As this has no notable effects on data interpretation, we have opted to use the original values for both datasets.

Standard deviation of multiple standards, analyzed in the same sample run, were 0.28‰ (SRM- 120c), 0.26‰ (*M. megalodon* tooth), and 0.17‰ (commercially available Sigma-Aldrich silver orthophosphate). We therefore assume a typical analytical uncertainty of 0.3‰ for the phosphate samples analyzed in this study.

3.3 Results and discussion

Isotope results are given in Table 3.2. For the neosalachian teeth, the average $\delta^{18}O_{sc}$ value is 26.8‰ ± 1.1‰ (SD), the average $\delta^{18}O_p$ value is 21.8‰ ± 1.9‰, and the average $\delta^{13}C$ value is 4.2 ± 3.1‰. There is no correlation between $\delta^{18}O_{sc}$ and $\delta^{18}O_p$ values (Fig. 3.1). Throughout the sampled geological sequence, $\delta^{18}O_p$ values span a relatively broad range without any apparent stratigraphic or species-specific trends (Fig. 2). Average *Allopleuron hofmanni* values are 27.0‰ ± 0.7‰ $\delta^{18}O_{sc}$, 20.2‰ ± 0.5‰ $\delta^{18}O_p$, and -5.6‰ ± 3.1 ‰ $\delta^{13}C$ (Table 3.2, Fig. 3.5, Fig. 3.6). The high standard deviation of the *A. hofmanni* $\delta^{13}C$ values is the result of an outlying cortical bone sample (1.6‰).

Table 3.2 Stable isotope compositions of late Maastrichtian and early Paleocene (early–middle Danian) shark and ray tooth enamel and *Allopleuron hofmanni* carapace bone. Carbon isotope ratios are given relative to VPDB, oxygen isotope values relative to VSMOW. Each sample number represents a different specimen. Teeth marked with an asterix were very small, and this may have resulted in dentin being sampled to some degree. For a detailed overview of stratigraphic levels, see W.M. Felder (1975) and Jagt and Jagt-Yazykova (2012).

#	species	stratigraphic level	$\delta^{13}C$	$\delta^{18}O_{sc}$	$\delta^{18}O_p$
1	*C. appendiculata pachyrhiza*	Geulhem Member, middle	5.1	25.7	22.1
2	*Palaeohypotodus bronni*	Geulhem Member, base	3.2	21.8	22.9
3	*Serratolamna serrata*	Meerssen, top	5.4	26.1	19.7
4	*Serratolamna serrata*	Meerssen, top	5.5	25.5	17.8
5 *	*Carcharias* sp.?	Meerssen Member, middle	-1.7	25.6	22.4
6 *	*Carcharias* sp.?	Meerssen Member, middle	-	-	20.6
7	*Palaeohypotodus bronni*	Meerssen Member, base	6.7	26.4	-
8	*Palaeohypotodus bronni*	Kanne horizon	3.7	27.1	-
9 *	*Palaeohypotodus bronni*	Kanne horizon	3.4	26.6	23.3
10 *	*Palaeohypotodus bronni*	Nekum Member, base	2.2	26.2	16.9
11 *	*Pseudocorax affinis*	Nekum Member, base	3.9	25.7	23.4
12	indeterminable	Emael Member, Lava horizon	4.1	27.3	19.6
13	indeterminable	Emael Member, Lava horizon	7.7	28.6	24.7
14 *	indeterminable	Emael Member, Lava horizon	6.8	27.3	21.0
15 *	*Palaeohypotodus bronni*	Emael Member, base	-1.7	26.7	17.8
16	*Pseudocorax affinis*	Emael Member, base	9.1	27.5	21.9
17 *	*Rhombodus binkhorsti*	Emael Member, base	3.9	26.7	23.3
18 *	*Palaeohypotodus bronni*	Emael Member, base	5.3	28.2	23.6
19 *	*Palaeohypotodus bronni*	Emael Member, base	-3.8	26.7	19.9
20	*Palaeohypotodus bronni*	Schiepersberg Member, base	4.6	26.0	24.5
21 *	*Palaeohypotodus bronni*	Schiepersberg Member, base	3.5	26.1	22.6
22 *	*Squalicorax pristodontus*	Gronsveld Member, base	1.7	26.8	23.0
23 *	*Ganopristis leptodon*	Gronsveld Member, base	-1.4	26.6	21.7
24 *	*Palaeohypotodus bronni*	Gronsveld Member, base	6.3	26.7	18.3
25	*Squalicorax pristodontus*	Valkenburg Member, base	3.0	26.5	22.3
26	*Palaeohypotodus bronni*	Valkenburg Member, base	5.7	28.0	-
27	*Pseudocorax affinis*	Valkenburg Member, base	6.8	27.9	23.4
28	*Palaeohypotodus bronni*	Valkenburg Member, base	11.0	27.9	20.8
29 *	*Pseudocorax affinis*	Valkenburg Member, base	6.5	27.0	22.2
30 *	*Palaeohypotodus bronni*	Valkenburg Member, base	3.4	26.5	23.1
31 *	indeterminable	Valkenburg Member, base	3.6	28.1	-
32	*Pseudocorax affinis*	Lanaye Member, top	7.1	28.2	23.4
33 *	*Pseudocorax affinis*	Lanaye Member, top	5.6	27.8	23.7

34 *	*Pseudocorax affinis*	Lanaye Member, top	5.3	27.7	22.2
35	*Squalicorax pristodontus*	Lanaye Member, base	7.9	26.9	21.5
36	*Palaeohypotodus bronni*	Lanaye Member, base	6.7	27.2	22.5
37	*Palaeohypotodus bronni*	Vijlen Member, middle	7.4	26.9	23.2
38	*Palaeohypotodus bronni*	Vijlen Member, base	2.7	26.8	20.2
39 *	*Palaeohypotodus bronni*	Vijlen Member, base	4.6	27.3	22.0
40 *	*Palaeohypotodus bronni*	Vijlen Member, base	0.9	25.9	24.2
41 *	*Centrophoroides appendiculatus*	Vijlen Member, base	-	-	21.7
42 *	*Centrophoroides appendiculatus*	Vijlen Member, base	-	-	20.3
43	*Anomotodon* sp.?	Kunrade Formation	1.6	26.4	22.7
44 *	*Palaeohypotodus bronni*	Kunrade Formation	0.0	26.7	22.2
45 I	*A. hofmanni* (cortical bone)	Maastrichtian, unknown layer	-7.5	26.8	20.4
45 II	*A. hofmanni* (cortical bone)	Maastrichtian, unknown layer	-6.8	27.1	20.8
45 III	*A. hofmanni* (cortical bone)	Maastrichtian, unknown layer	-7.1	26.2	20.4
45 IV	*A. hofmanni* (cortical bone)	Maastrichtian, unknown layer	-6.9	26.5	20.5
45 V	*A. hofmanni* (cancellous bone)	Maastrichtian, unknown layer	1.6	26.5	20.5
45 VI	*A. hofmanni* (cancellous bone)	Maastrichtian, unknown layer	-4.0	28.5	19.9
45 VII	*A. hofmanni* (cancellous bone)	Maastrichtian, unknown layer	-7.2	27.3	19.2
45 VIII	*A. hofmanni* (cancellous bone)	Maastrichtian, unknown layer	-7.2	27.1	-

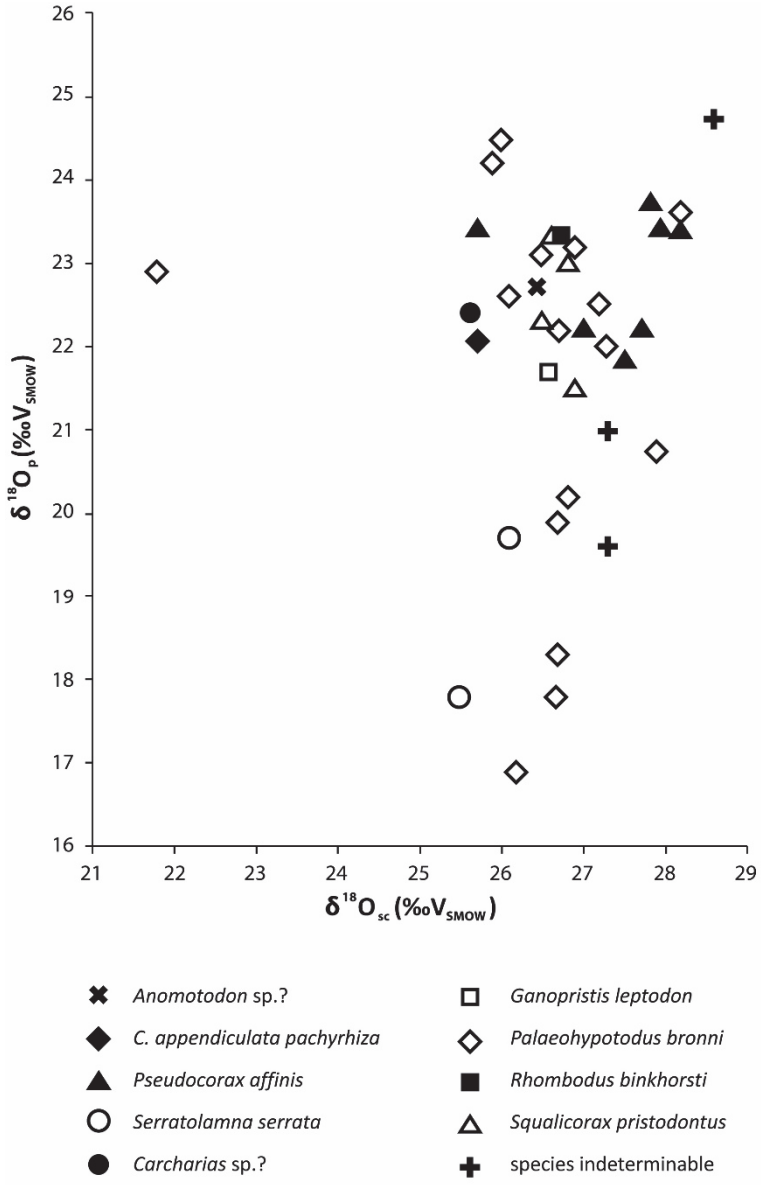

Figure 3.1 Oxygen isotope compositions of shark and ray tooth enamel from the Maastrichtian type area: structural carbonate ($\delta^{18}O_{sc}$) fraction versus phosphate ($\delta^{18}O_{p}$) fraction.

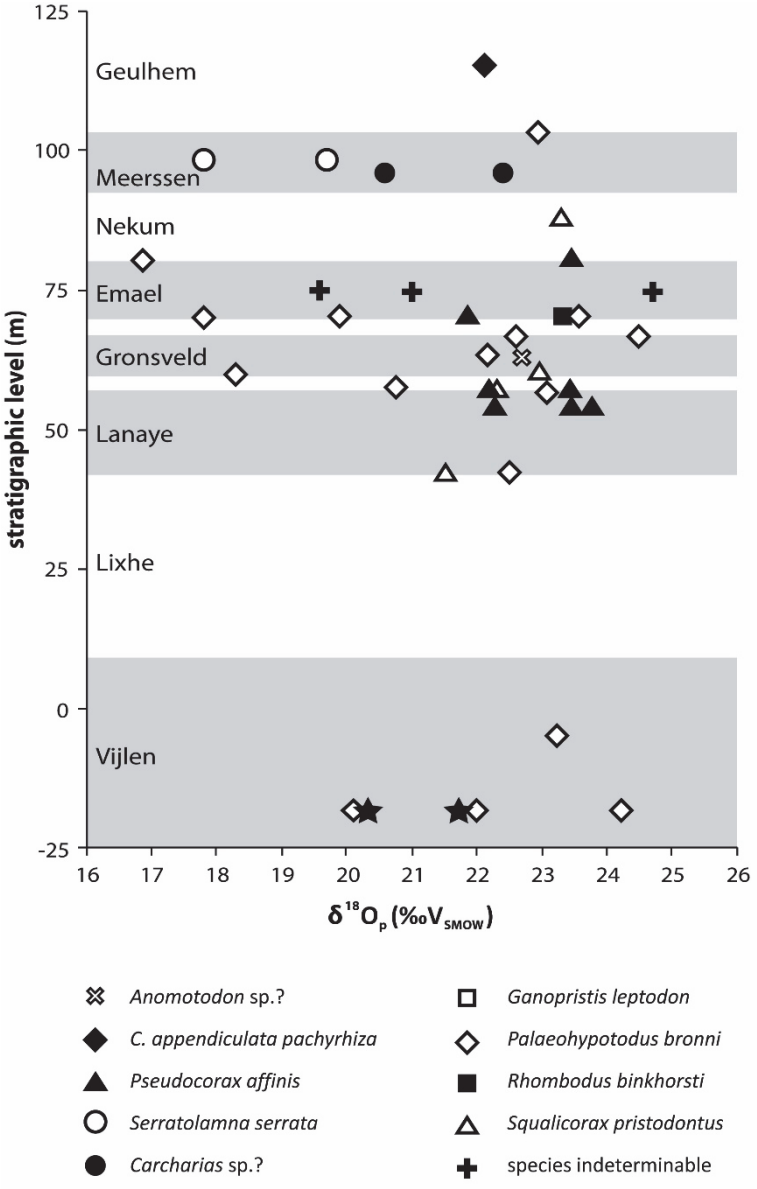

Figure 3.2 Shark and ray tooth enamel $\delta^{18}O_p$ values plotted per species, versus stratigraphic level. Name and thickness of stratigraphic members are after Jagt and Jagt-Yazykova (2012): situated between the Lanaye and Gronsveld Members is the Valkenburg Member, and between the Gronsveld and Emael Members is the Schiepersberg Member. The stratigraphic level of 0 m is the current quarry floor at the ENCI–Heidelberg Cement Group quarry, Maastricht. The stratigraphic position of the two shark teeth from the Kunrade Formation (*Anomotodon* sp. and *Palaeohypotodus bronni*) was extrapolated to fit the ENCI quarry stratigraphy (at 63 m in this graph).

3.3.1 Comparison to a modern dataset

In contrast to most other fossil species found in the Maastrichtian type area, late Maastrichtian and early Paleocene shark and ray teeth can be compared to modern counterparts. We make this comparison on the basis of tooth isotope data from extant subtropical sharks caught off the coast of South Africa, published by Vennemann et al. (2001) (Fig. 3.3, Fig. 3.4). This dataset comprises 15 individual sharks belonging to the species *Carcharias brevipinna, Carcharias carcharias, Carcharias taurus, Carcharhinus limbatus, Carcharhinus obscurus, Galeocerdo cuvier, Isurus oxyrhincus*, and *Sphyrna mokarran*. Where applicable, the values of multiple samples are averaged per individual shark.

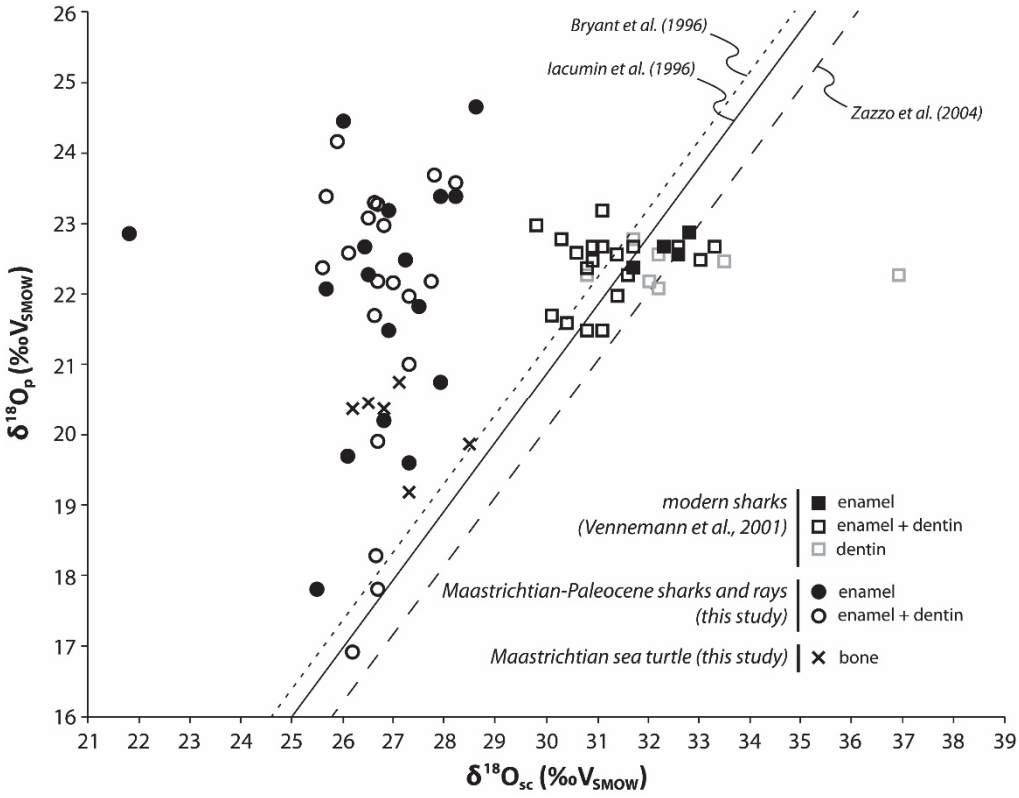

Figure 3.3 Shark, ray, and turtle $\delta^{18}O_{sc}$ and $\delta^{18}O_p$ data presented in this study, compared to shark $\delta^{18}O_{sc}$ and $\delta^{18}O_p$ data by Vennemann et al. (2001). Also given are best fit lines for $\delta^{18}O_{sc}$ versus $\delta^{18}O_p$ correlations found for modern horses (Bryant et al., 1996), modern mammals from various species (Iacumin et al., 1996), and Miocene-Pliocene hypsodonts (Zazzo et al., 2004).

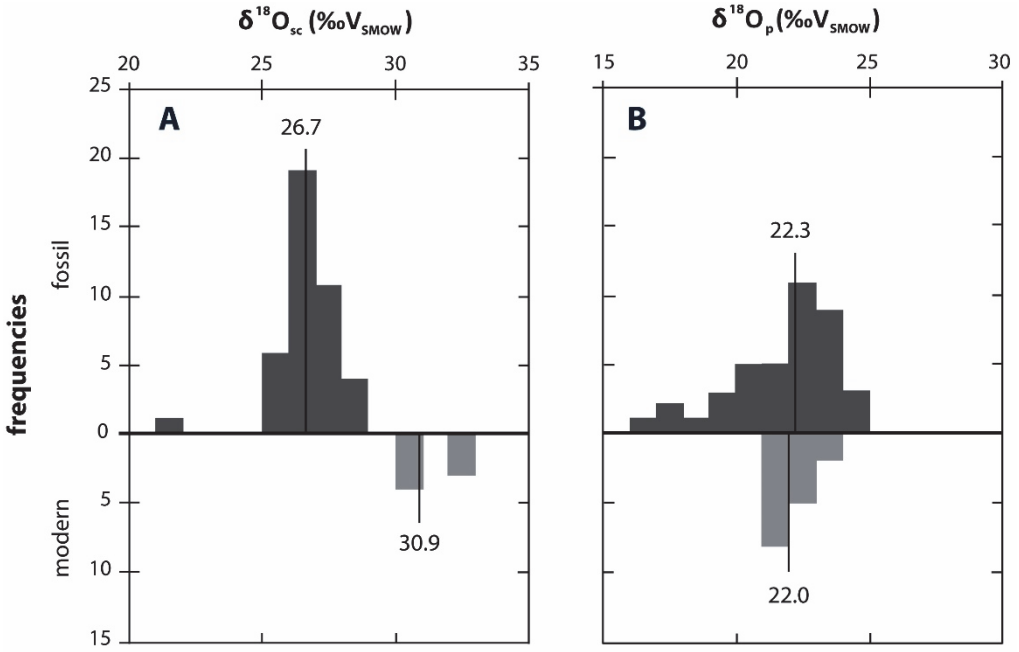

Figure 3.4 Histograms of shark and ray $\delta^{18}O_{sc}$ and $\delta^{18}O_p$ data. Median values are shown for each frequency distribution. Upper panels show all samples from Maastrichtian and Paleocene sharks and rays. Lower panels show samples from extant sharks as measured by Vennemann et al. (2001), from which we selected all samples described as 'enamel' and 'top of tooth'.

3.3.2 Neosalachian $\delta^{18}O$ values

The Maastrichtian-Paleocene $\delta^{18}O_p$ data (median value 22.3‰) compares well to a Maastrichtian fish tooth from the same stratigraphic sequence (22.3‰) analyzed by Pucéat et al. (2007) and to modern shark tooth $\delta^{18}O_p$ as presented by Vennemann et al. (2001) (22.0‰) (Fig. 3.4B). The fossil neoselachian data does deviate from a Gaussian frequency distribution, with a small but distinct cluster of low $\delta^{18}O_p$ values. We found no independent geochemical or preservation-related evidence to discard these samples, and on this basis include them in further comparisons and calculations on the entire dataset (exclusion would shift the median $\delta^{18}O_p$ value by only 0.15‰).

Whether we include or exclude these lowest $\delta^{18}O_p$ values, the fossil neoselachians display a slightly wider range than the modern sharks (Fig. 3.4B). This is not surprising, as these teeth originate from a ~4 million year interval compared to the 4-year period (1996–1999) covered by the Vennemann et al. (2001) dataset. Every single stratigraphic level represents a

considerable time span (Jagt and Jagt-Yazykova, 2012), for which we find up to 2.2‰ $\delta^{18}O_p$ variation (compared to 1.4‰ for modern sharks).

As for the Maastrichtian-Paleocene $\delta^{18}O_{sc}$ data, comparison with modern sharks (Fig. 3.4A) reveals an offset of ~5-6‰. Approximately ~1‰ of that offset can be accounted for by the fact that there existed no ice caps during the Maastrichtian and early Paleocene, resulting in lower ocean $\delta^{18}O$ values (Shackleton and Kennett, 1975). We propose that the remaining offset is likely due to meteoric diagenesis. Vonhof et al. (2011) reports a ~1-2‰ diagenetic $\delta^{18}O$ shift towards lower values for type Maastrichtian belemnites, with the lowest altered $\delta^{18}O_{calcite}$ value being -2.7‰ V_{PDB}, or 28.1‰ V_{SMOW}. The fact that the majority of our shark and ray $\delta^{18}O_{sc}$ data has similar values suggests that the teeth may have been diagenetically completely overprinted.

This interpretation is further strengthened by the fact that the data exhibits no correlation between $\delta^{18}O_{sc}$ and $\delta^{18}O_p$ values (Fig. 3.3). Modern mammals display a strong correlation between the oxygen isotope compositions of these two fractions, with a fixed difference of ~9-10‰ (Bryant et al., 1996; Iacumin et al., 1996; Zazzo et al., 2004; Pellegrini et al., 2011), and $\delta^{18}O_p$ has proven to be more resistant to inorganic diagenetic alteration than $\delta^{18}O_{sc}$ (Tudge, 1960; Kolodny et al., 1983; Zazzo et al., 2004). Paired $\delta^{18}O_p$ and $\delta^{18}O_{sc}$ analyses on biogenic apatite may therefore be used to assess the extent of diagenetic alteration of fossil bone and tooth material (Stanton Thomas and Carlson, 2004; Zazzo et al., 2004). Figure 3.3 shows that the subtropical sharks in the dataset of Vennemann et al. (2001) plot in close proximity to the calculated best fit lines determined for modern mammals, with an average offset of 9.2 ± 1.3‰ (n = 34). In contrast, the oxygen isotope values of Maastrichtian and Paleocene neosalachian teeth display a $\delta^{18}O_p$ versus $\delta^{18}O_{sc}$ offset of 4.8 ± 2.1‰ (n = 37). Note that both in the Maastrichtian-Paleocene and the modern neosalachians, samples that contain some amount of dentin do not deviate in $\delta^{18}O$ values from samples consisting purely of enamel, i.e. dentin admixture is not a cause of variability in the $\delta^{18}O_p$ versus $\delta^{18}O_{sc}$ offset.

3.3.3 Paleotemperature calculation

Based on the diagenetic robustness of phosphate oxygen in general, and the good agreement of the measured values with those of modern sharks and the Maastrichtian fish tooth analyzed by Pucéat et al. (2007), we surmise that the Maastrichtian and Paleocene neoselachian teeth yield *in vivo* $\delta^{18}O_p$ values. Based on these values, paleo-seawater temperature can be calculated using the phosphate–water fractionation equation for biogenic apatite by Pucéat et al. (2010) (which assumes a value of 22.6‰ δ18Op for NIST SRM 120c, equal to the value we used for standardization):

$T = 124.6 - 4.52 \times (\delta^{18}O_p - \delta^{18}O_w)$ (equation 2)

Based on the median tooth enamel $\delta^{18}O_p$ value of 22.3‰ and a Maastrichtian $\delta^{18}O_w$ value of −1‰ V_{SMOW} (Shackleton and Kennett, 1975), we calculate a water temperature of 19.3°C. This is in good agreement with Late Maastrichtian sea surface temperatures in this region, as calculated in earlier work: Lowenstam and Epstein (1954) comes to a temperature of 18°C based on belemnite rostra, and Zakharov et al. (2006) finds a temperature of 19.8°C based on a bivalve shell.

However, if we calculate water temperatures for the entire range of measured $\delta^{18}O_p$ values, the result indicates an unrealistic amount of temperature variation: approximately 8 to 44 °C. Seasonal thermal fluctuations and a vertical ocean water temperature gradient could have caused some, but not all of this variation. Instead, the broad $\delta^{18}O_p$ range may predominantly be a reflection of significant spatial (as well as temporal) variation in $\delta^{18}O_w$, perhaps tied to evaporation off shallow parts of the Maastrichtian sea (see Pucéat et al., 2003) and the influx of freshwater from the nearby Rhenish Massif.

3.3.4 Marine turtle $\delta^{18}O$ values

Similarly to the fossil neosalachian specimens, $\delta^{18}O_{sc}$ and $\delta^{18}O_p$ values of the *Allopleuron hofmanni* carapace bone samples are offset from the correlation lines found by Bryant et al. (1996), Iacumin et al. (1996), and Zazzo et al. (2004) (Fig. 3.3). The *A. hofmanni* $\delta^{18}O_{sc}$ values thus do not seem to represent *in vivo* values.

In contrast, the original $\delta^{18}O_p$ values of dense cortical bone may well be preserved in material of this age (Barrick, 1998; Barrick and Showers, 1999). *A. hofmanni* cortical bone $\delta^{18}O_p$ values fall within a narrow range of 20.5 ± 0.2‰ V_{SMOW}, while the cancellous bone shows a trend towards lower values away from the compact bone (Fig. 3.5). This possibly indicates diagenetic alteration of the more porous and permeable bone tissue. Barrick et al. (1999) and Coulson et al. (2008) found that modern turtle species precipitate bone within the same narrow temperature range, with the correlation between bone $\delta^{18}O_p$ and host water $\delta^{18}O_w$ being:

$\delta^{18}O_w = 1.06 (\pm 0.06) \times \delta^{18}O_p - 22.7 (\pm 1.3)$ (equation 3)

Inserting in this equation a $\delta^{18}O_p$ value of 20.5‰ results in a paleo-$\delta^{18}O_w$ value of −1.0‰. The total range of cortical bone $\delta^{18}O_p$ values represents $\delta^{18}O_w$ values of -1.1 to -0.7‰. These realistic $\delta^{18}O_w$ values further support the hypothesis that the phosphate oxygen in the *A. hofmanni* cortical bone has not been diagenetically altered.

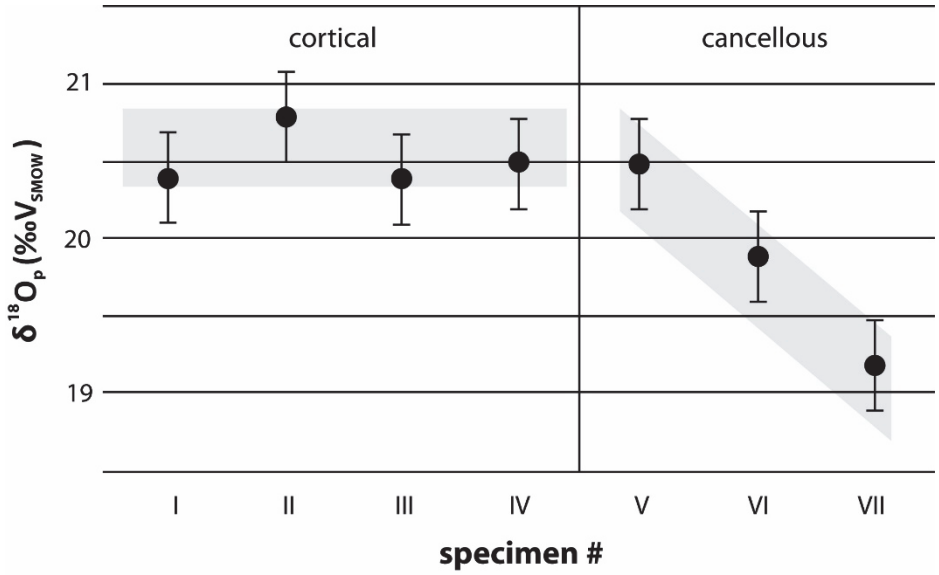

Figure 3.5 Marine turtle *Allopleuron hofmanni* $\delta^{18}O_p$ values from a dorsoventral growth line (sclerochronological) series of carapace bone (NHMM 2008 137).

3.3.5 Neosalachian $\delta^{13}C$ values

Carbon isotope values for Maastrichtian and Paleocene neosalachian teeth span a broad range of ~15‰. We found no clear species-specific trends. *Palaeohypotodus* bronni plots throughout the entire range (-3.8 to 11.0‰). *Squalicorax pristodontus* (1.7 to 7.9‰) and *Pseudocorax affinis* (3.9 to 9.1‰) also cover a broad range of values.

Within the Maastrichtian-Paleocene dataset, there is an offset between the $\delta^{13}C$ values of very small teeth, samples of which likely contain dentin as well as enamel (2.8 ± 3.0‰ $\delta^{13}C$), and larger teeth (5.8 ± 2.3‰ $\delta^{13}C$) (Fig. 3.6). This offset is not the result of the smaller teeth belonging to other species than the larger teeth, as there is no correlation between $\delta^{13}C$ value and species designation. Vennemann et al. (2001) finds a similar $\delta^{13}C$ difference between whole teeth samples and samples only consisting of enamel, and suggests secondary diffusional processes and isotopic exchange with seawater DIC as likely explanations for this offset.

A significant part of both datasets consists of the 'enamel + dentin' category, which likely encompasses mixtures with very different proportions of enamel versus dentin, and is therefore not ideal for comparison. Yet (also taking into account the pure enamel samples) Maastrichtian and Paleocene neosalachian teeth show an offset of ~3-6‰ towards more positive $\delta^{13}C$ values compared to the extant shark teeth. We hypothesize that this is due to a

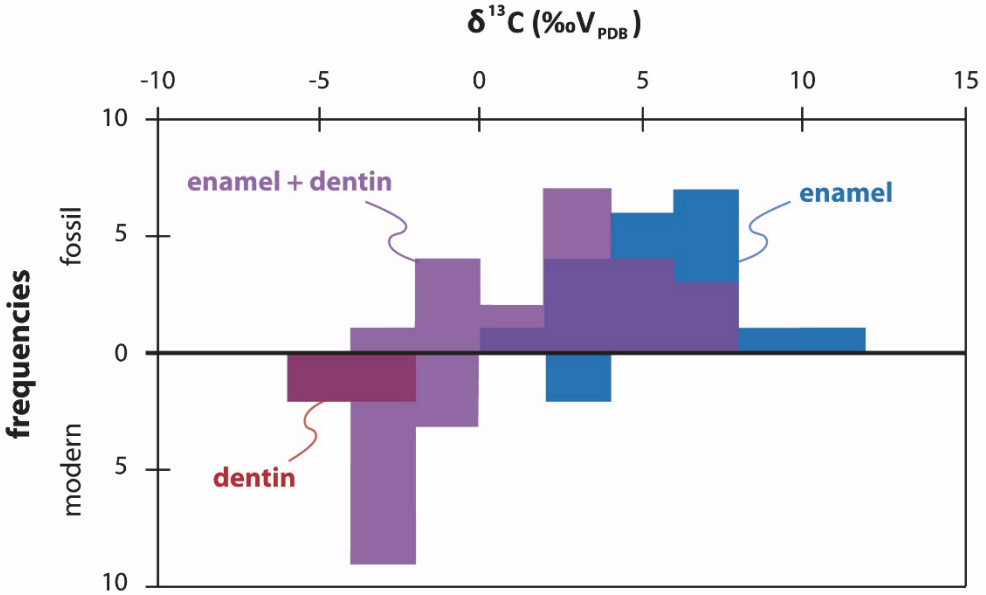

Figure 3.6 Histograms of shark and ray $\delta^{13}C$ data, per type of tooth material. Upper panel shows samples from Maastrichtian and Paleocene sharks and rays. Lower panel shows extant sharks, as measured by Vennemann et al. (2001), with the 'enamel + dentin' category consisting of any sample that is not labelled as 'enamel' or 'dentin' (i.e. 'whole tooth', 'top of tooth').

difference in the $\delta^{13}C$ values at the base of the food chain, possibly tied to the possibility that Maastrichtian and Paleocene neosalachians were feeding in even warmer waters than the extant sharks caught off the coast of South-Africa (Sackett, 1989; Vennemann et al., 2001).

3.3.6 Marine turtle $\delta^{13}C$ values

The average $\delta^{13}C$ value for *A. hofmanni* cortical bone is −7.1 ± 0.3‰. Cancellous bone values are in a similar range, except for one conspicuous outlier (1.6‰) that may have resulted from the inclusion of secondary carbonate accretions into the sample. Bone is less resistant to diagenetic influences than tooth enamel, but complete diagenetic overprinting is unlikely for this sample, since the measured $\delta^{13}C$ value is ~7‰ lower than the values generally reported for belemnites, foraminifera and diagenetic calcites from the type Maastrichtian (Barrera et al., 1997; Friedrich et al., 2009; Vonhof et al., 2011). As diagenesis would be expected to draw $\delta^{13}C$ to higher values, we deduce that the original $\delta^{13}C$ values of the *A. hofmanni* bone cannot have been higher than ~ -7‰. As shown in Fig. 3.7, these values are in agreement with $\delta^{13}C$ values of extant marine turtles such as *Dermochelys coriacea* and *Lepidochelys olivacea*. They

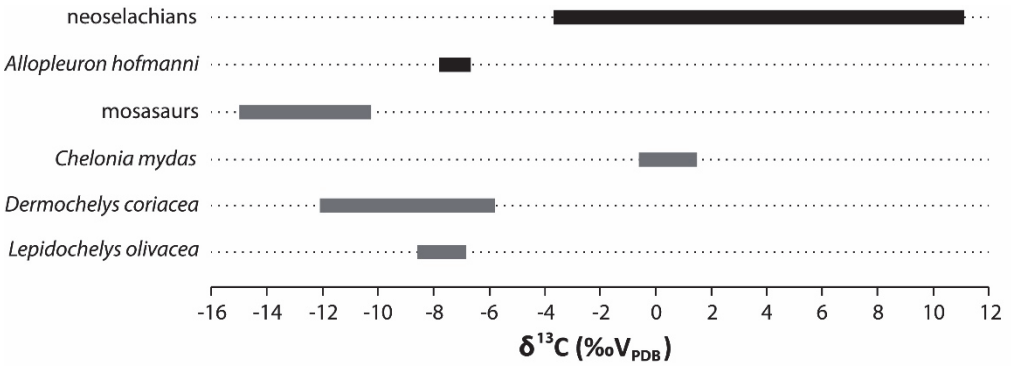

Figure 3.7 $\delta^{13}C$ values of neoselachians (this study), *Allopleuron hofmanni* (this study) and sympatric mosasaurs (Schulp et al., 2013), as well as several extant marine turtles (carnivorous *Dermochelys coriacea* and *Lepidochelys olivacea*, and herbivorous *Chelonia mydas*; see Biasatti, 2004).

contrast with the ~8‰ higher values for the marine turtle *Chelonia mydas*, which is due to the high dietary proportion of seagrass (Hemminga and Mateo, 1996; Biasatti, 2004).

Interpretation of *Allopleuron hofmanni* $\delta^{13}C$ values is complicated by the fact that marine turtle bone $\delta^{13}C$ is determined by two major factors: diet and respiratory physiology. An enrichment of 12‰ or more can be expected between a herbivorous diet and bone carbonate, whereas a carnivorous diet will result in enrichment of 6-9‰ (Biasatti, 2004). As for respiratory physiology: when lung-breathing (pulmonate) marine reptiles such as turtles and mosasaurs dive, they need to hold their breath. Accumulation of respired CO_2, which is depleted in ^{13}C (McConnaughey et al., 1997), causes the $\delta^{13}C$ incorporated in the tissues of marine pulmonates to be lower than in gill-breathing fish (Biasatti, 2004; Robbins et al., 2008; Schulp et al., 2013). This explains why the neoselachian $\delta^{13}C$ values we measured in this study are ~18‰ higher than mosasaur $\delta^{13}C$ values measured by Schulp et al. (2013) (Fig. 3.7).

As a result, there are several pathways which can result in a carbon isotope composition of -7‰ $\delta^{13}C$ in marine turtle bone. At one end of the spectrum, *A. hofmanni* only engaged in dives of a short duration (rendering the effect of respiratory CO_2 accumulation negligible). In this case, its diet would consist of foodstuffs with $\delta^{13}C$ values of ~-19‰ (for a completely herbivorous diet) to ~-13‰ (for a completely carnivorous diet). A herbivorous diet for *A. hofmanni* would likely consist of seagrass: there is fossil evidence for the existence of seagrass meadows in the Maastrichtian stratotype area (*Thallassotaenia debeyi*; Voigt and Domke, 1955; Van der Ham et al., 2007) and this has been hypothesized as a food source for *A. hofmanni* (Chapter 2 of this thesis; Janssen et al., 2011). In view of the range of $\delta^{13}C$ values encountered in extant species of seagrass (Hemminga and Mateo, 1996), a fully herbivorous diet for *A. hofmanni* would imply that *T. debeyi* exhibited relatively low (but still feasible) $\delta^{13}C$

values for a seagrass species. A fully carnivorous diet of -13‰ $\delta^{13}C$ is a also a realistic possibility under these circumstances, considering the $\delta^{13}C$ range of common animal food sources for turtles (see Fig. 3.4 in Biasatti, 2004) and the presence of relatively high $\delta^{13}C$ values in (part of) the Maastrichtian and Paleocene ecosystems (see section 3.3.5).

Conversely, at the other end of the spectrum, *A. hofmanni* did frequently engage in dives of long duration, drawing down $\delta^{13}C$ values considerably. This would allow for seagrass $\delta^{13}C$ values more typical observed in extant seagrass species. However, it is not evident why a marine turtle with a diet primarily based on seagrass would regularly perform long dives, as seagrass needs a favorable light environment for growth and thus only thrives on relatively shallow seabeds. Additionally, in case of a predominantly carnivorous diet we would have to assume unrealistically high $\delta^{13}C$ values for animal food sources.

3.4 Conclusions

The examined neoselachian teeth from the upper Maastrichtian and lower Paleocene of the Maastrichtian type area appear to have retained *in vivo* $\delta^{18}O_p$ values, while $\delta^{18}O_{sc}$ values have likely been depleted due to meteoric diagenesis. Based on a median value of 22.3‰ $\delta^{18}O_p$ for these samples we calculate an average Maastrichtian seawater temperature of 19.3 °C, which is in good agreement with previous estimates for this region. However, the wide range in tooth enamel $\delta^{18}O_p$ values cannot have been caused by temperature variation alone: we propose spatial variations in $\delta^{18}O_w$ to be an additional factor. Our results underscore that paleotemperature reconstruction based on individual specimens carries a relatively high degree of uncertainty, and that comprehensive sampling is necessary to capture the variations in such a dynamic system.

The carbon isotope compositions of Maastrichtian and Paleocene neosalachians presented in this study display a difference between dentin and enamel similar to that of extant sharks (Vennemann et al., 2001), corroborating the hypothesis that this offset is a species-independent feature occurring in all sharks. The overall offset towards more enriched $\delta^{13}C$ values shows that carbon isotope ratios were relatively high in the ecosystem represented by the type Maastrichtian, a finding that should be taken into account when evaluating the carbon isotope composition of other species from this area.

Based on the $\delta^{13}C$ values of *Allopleuron hofmanni* we surmise that it is unlikely that this marine turtle has engaged in frequent and long-duration dives. The data do not allow us to distinguish between a carnivorous or herbivorous diet, although the latter is only feasible if we assume comparatively low $\delta^{13}C$ values for the seagrass species *Thallassotaenia debeyi*. Carbon isotope measurements of fossil *T. debeyi* specimens would theoretically allow us to test if *Allopleuron hofmanni* had a herbivorous diet, but based on the descriptions by (Voigt

and Domke, 1955; Van der Ham et al., 2007) but it is unlikely that these rare specimens have been sufficiently preserved to allow for reliable $\delta^{13}C$ measurements.